

Spiral waves in linearly coupled reaction-diffusion systems

Hujiang Yang^{1,2} and Junzhong Yang^{1,*}

¹*School of Science, Beijing University of Posts and Telecommunications, Beijing, 100088, People's Republic of China*

²*Department of Physics, Beijing Normal University, Beijing, 100875, People's Republic of China*

(Received 1 October 2006; revised manuscript received 2 January 2007; published 10 July 2007)

The dynamics of spiral waves in a pair of linearly coupled reaction-diffusion systems is investigated. We find that the spiral dynamics depends on the coupling strength between the two subsystems. When the coupling strength is weak, the frequency and wavelength of the spiral wave in each subsystem remain unchanged. The interaction between the two subsystems induces the drift of spiral waves. When the coupling strength is strong, synchronization between the two subsystems is established. The two subsystems play different roles in the collective dynamics: one subsystem is always dominant and enslaves the other.

DOI: [10.1103/PhysRevE.76.016206](https://doi.org/10.1103/PhysRevE.76.016206)

PACS number(s): 05.45.-a, 47.54.-r, 82.40.Ck

INTRODUCTION

Spiral waves are the most frequently encountered pattern formation in two-dimensional (2D) systems driven away from equilibrium. They are usually thought to be responsible for the patterns in a wide range of systems, from chemical reactions [1] and physiological media [2] to slime aggregates [3] and hydrodynamics [4]. In addition, spiral waves can display a number of distinct behaviors, some of which are quite complex. The simplest transition in spiral waves is Hopf bifurcation, which turns a rigidly rotating spiral wave (that is, periodic) into a quasiperiodic meandering one [5,6] where the distances between consecutive spiral arms are expanded and contracted. Another common transition is the breakup of spiral waves, which comes in two different ways: the core or far field breakup. In core breakup, the spiral wave develops into turbulence first near the spiral core and the mechanism behind it is attributed to the Doppler effects [7,8]. In far field breakup, spiral waves first become unstable far away from the core and the instability underlying this transition is the absolute Eckhaus one [9,10].

Most real systems we encounter are three dimensional, for example, intensively investigated cardiac tissues [11] and chemical reaction systems. Studies on scroll waves, the counterparts of spiral waves in 3D systems, have shown that there exists a critical thickness in the direction of the third dimension for the onset of 3D effects [12], which means that the 3D effects can be ignored if the medium is thin enough and the 3D system can be approximated by a 2D one. However, in chemical reaction systems such as the Belousov-Zhabotinsky reaction, there always exists a parameter gradient across the reaction layer [13]. Therefore, though the reaction layer may be thin enough that the 3D effects can be ignored, we still cannot treat such a system as a simple 2D one. Instead of the 2D or 3D description, a possible way to handle this kind of system is to consider them as coupled 2D systems [14].

In this paper we will investigate the spiral wave dynamics in linearly coupled 2D reaction diffusion systems where the subsystems have different parameters. Such a configuration

is also significant in the field of nonlinear dynamics. For example, in coupled nonidentical low-dimensional systems such as coupled phase oscillators or chaotic oscillators, it is well known that the different oscillators will reach the state of phase synchronization when the coupling strength is strong enough [15]. The transition to phase synchronization is always characterized by a continuous process: the rotation velocities of different oscillators match each other gradually with the increase of the coupling strength. However, for coupled extended systems displaying spiral waves to reach phase synchronization, they have to adjust both temporal and spatial periodicities in a consistent way. Therefore, it is interesting to investigate what happens for spiral dynamics when two extended systems with different parameters are coupled.

In this work, we find that there are two fundamental types of spiral dynamics in coupled reaction-diffusion systems. When the coupling strength between the two subsystems is weak, the interaction between them only induces the drifts of spiral waves without changing the functional forms of the spiral waves. When the coupling strength is strong enough, phase synchronization between the two subsystems is established. Unlike phase synchronization in coupled low-dimensional systems, the two subsystems will play different roles in the collective dynamics: one subsystem always behaves like a leader while the other one follows the leader on both rotating frequency and wavelength. For intermediate coupling strength, a transition process is readily found where the spiral wave of the follower is driven out of the domain and the leader takes over the follower's dynamics gradually by embedding its spiral wave in the follower.

THE MODEL

We consider coupled reaction-diffusion systems with no-flux boundary condition where the local dynamics is proposed by Bär and Eiswirth [7]. The model in the dimensionless form is described as

$$\partial u_1 / \partial t = f_1(u_1, v_1) + \Delta u_1 + c(u_2 - u_1),$$

$$\partial v_1 / \partial t = g_1(u_1, v_1),$$

$$\partial u_2 / \partial t = f_2(u_2, v_2) + \Delta u_2 + c(u_1 - u_2),$$

*jzyang@bupt.edu.cn

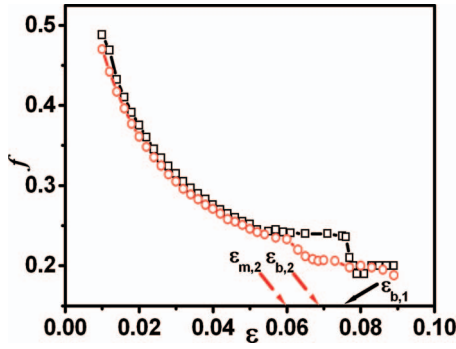


FIG. 1. (Color online) Rotating frequency of spiral wave vs ϵ . The parameter $b = -0.045$ (open squares) and 0.05 (open circles). $\epsilon_{b,1}$ and $\epsilon_{b,2}$ denote the spiral wave breakup for $b = -0.045$ and 0.05 , respectively. $\epsilon_{m,2}$ denotes the meandering transition for $b = 0.05$. The transition scenario for $b = -0.045$ is a little complicated as can be found in Ref. [16].

$$\partial v_2 / \partial t = g_2(u_2, v_2),$$

$$f_{1,2}(u, v) = -u(u-1)[u - (v + b_{1,2})/a_{1,2}]/\epsilon_{1,2},$$

$$g_{1,2}(u, v) = \begin{cases} -v & \text{if } u < \frac{1}{3}, \\ 1 - 6.75u(u-1)^2 - v & \text{if } \frac{1}{3} < u < 1, \\ 1 - v & \text{if } u > 1, \end{cases} \quad (1)$$

where $\Delta = \partial^2 / \partial x^2 + \partial^2 / \partial y^2$. To numerically simulate the coupled systems, we use the forward Euler method with $dt = 0.015$ and $\Delta x = \Delta y = 0.3$. The system size is set to be $N\Delta x \times N\Delta y$ where $N = 200$ (the main results do not depend on the discretization scheme and the size of the system). Throughout the paper, we take the parameters $a_{1,2}$ to be constant ($a_{1,2} = 0.84$). The local dynamics can be changed from excitable to oscillatory when we change the parameter $b_{1,2}$ from positive to negative. For any given $b_{1,2}$, the isolated 2D system may undergo transitions from a rigidly rotating spiral wave to spiral wave breakup [10,16] when $\epsilon_{1,2}$ is increased. During the transitions, the rotating frequency of the spiral wave always decreases with increasing ϵ whether the medium is excitable ($b = 0.05$) or oscillatory ($b = -0.045$) as shown in Fig. 1 (for a meandering spiral wave and spiral wave breakup, the frequency with the highest amplitude is recorded [17]). The two curves shown in Fig. 1 are quite similar except for the sharp dip for $b = -0.045$. The sharp dip at $\epsilon = 0.078$ indicates the spiral wave breakup. According to Refs. [10,16], the breakup of the spiral wave here belongs to the far field one. The discontinuity of the frequency at $\epsilon = 0.078$ could be explained by the fact that the breakup of the spiral wave is caused by an absolute Eckhaus instability [18]. The wave train emitted by the spiral core becomes linearly unstable when the convective instability sets in. At the same time the resulting turbulence is invisible since it propagates outside the system. The turbulence observed after the onset of the absolute Eckhaus instability is not a direct consequence of the absolute instability, which is the reason for the

appearance of the dip in the curve of frequency. On the contrary, for $b = 0.05$, the spiral breakup occurs first near the spiral core and the resulting turbulence is created directly from the previous spiral wave. Therefore, no discontinuity appears in frequency in this case.

THE DRIFT OF SPIRAL WAVES

Generally, there are two regimes for the coupled spiral dynamics. When the coupling strength is very weak, the two spiral waves keep their dynamics almost unchanged in respect of their frequencies and wavelengths whether the spiral waves are rigidly rotating or meandering. The effects of the interaction between the two subsystems are disclosed through the movement of the spiral tips. Two typical situations are classified according to the frequency mismatch between the two spiral waves. We first consider the case where spiral waves in isolated subsystems have large mismatch in their rotating frequencies (nonresonant case). We let $b_1 = -0.045$, $\epsilon_1 = 0.012$, $b_2 = -0.045$, and $\epsilon_2 = 0.036$. Under these parameters, the spiral waves in the isolated subsystems are rigidly rotating ones. As shown in Fig. 1, the rotating frequency in subsystem 1 is around 0.48 and that in subsystem 2 is around 0.29. By using these rigidly rotating spiral waves in the isolated systems as initial conditions, the spiral waves in coupled systems are generated. When $c = 0.0012$, the power spectra for the two subsystems before and after the interaction is switched on are shown in Figs. 2(a) and 2(b) where we can see that the rotating frequencies of the two spiral waves are the same as the isolated ones. The snapshots of the spiral waves for the isolated systems and the coupled systems after the transient are shown in Figs. 2(c) and 2(d). The characteristics of the wave patterns such as the wavelength seem unchanged too. Nevertheless, comparing the snapshots carefully, we may notice that the rotation center of the spiral wave in subsystem 1 stays very close to its original location while that of subsystem 2 shifts away. The tip trajectories presented in the top panel in Figs. 3(a) and 3(b) show clearly that the tip in subsystem 2 has jumped to a large looped orbit while the spiral tip in subsystem 1 stays in a small orbit close to its original one. Further simulations reveal the following observations: (1) The tip trajectories in the two subsystems are independent of the coupling strength if the coupling strength is not strong; (2) the tip trajectories in the two subsystems are concentric; (3) the moving velocity of the spiral tip along the looped orbit in subsystem 2 increases with the coupling strength by a power law. As shown in Fig. 3(c), the slope in the log-log plot is around 2. From Fig. 3(c), we know that the drifting velocity is much lower, which means that the secondary frequency induced by the spiral drifting is much smaller than that of the original spiral wave. For example, the secondary frequency induced by drifting at $c = 0.0012$ is around $f_{in} = 2 \times 10^{-4}$. Comparing with $f_1 = 0.48$ and $f_2 = 0.29$, the secondary frequency is extremely small. Consequently, the secondary frequency f_{in} is not visible in the power spectrum shown in Fig. 3(b).

Now we consider the other case where the mismatch between the frequencies of the two spiral waves is very small (the resonant case). To investigate it, we let $b_1 = -0.045$, ϵ_1

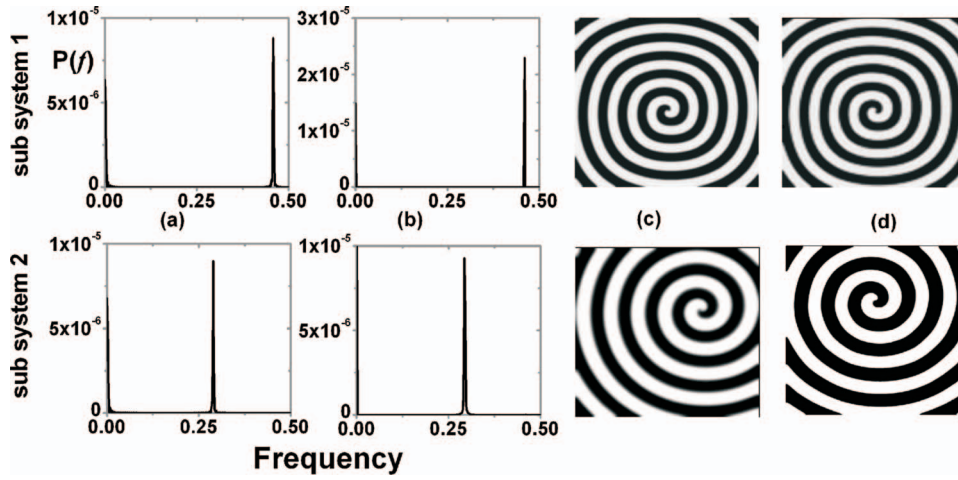


FIG. 2. Power spectra for two subsystems when they are isolated (a) or coupled together in a linear way with $c=0.0012$ (b); snapshots for the two subsystems are plotted when they are isolated (c) or coupled together (d). The top panel is for subsystem 1 $b_1=-0.045$ and $\epsilon_1=0.012$; the bottom panel is for subsystem 2 $b_2=-0.045$ and $\epsilon_2=0.036$.

$=0.022$, $b_2=0.05$, and $\epsilon_2=0.02$. From Fig. 1, we know that the rotating frequencies for the two subsystems are almost the same ($f_1=0.36$ and $f_2=0.361$). Unlike the nonresonant case where the spiral waves in the two subsystems drift in different orbits, the tip trajectories for both subsystems in the resonant case fall into the same orbit, as shown in the bottom panel in Figs. 3(a) and 3(b). (The difference in the widths of the orbits for two spiral waves is due to the difference in the diameters of the circular orbits when they are isolated.) It should be noted that the spiral waves in both subsystems are not in synchronization. First, the spiral tips of the two subsystems move along the same orbit with a time lag; second, the spiral waves in the two subsystems preserve their original frequencies and wavelengths. The moving velocity of the spiral tips along the orbit also increases with the coupling

strength, but in a piecewise linear way [see the bottom panel in Fig. 3(c)].

Further simulations for different parameters b_i and ϵ_i show that, in the nonresonant case, the subsystem with the spiral tip moving along the large looped orbit is the one with the slow rotating spiral wave. The simulations also show that the parameter regime for the resonant case is too narrow to make a clear boundary for it. In particular, if we change parameters to within the resonant case away from the nonresonant one, we can find some other types of spiral drifting dynamics when the parameters are close to the resonant situation. For example, spiral tips in both subsystems may drift along the boundary or perform some erratic motions.

We now present heuristically an ordinary differential equation model, which can explain some of the numerical

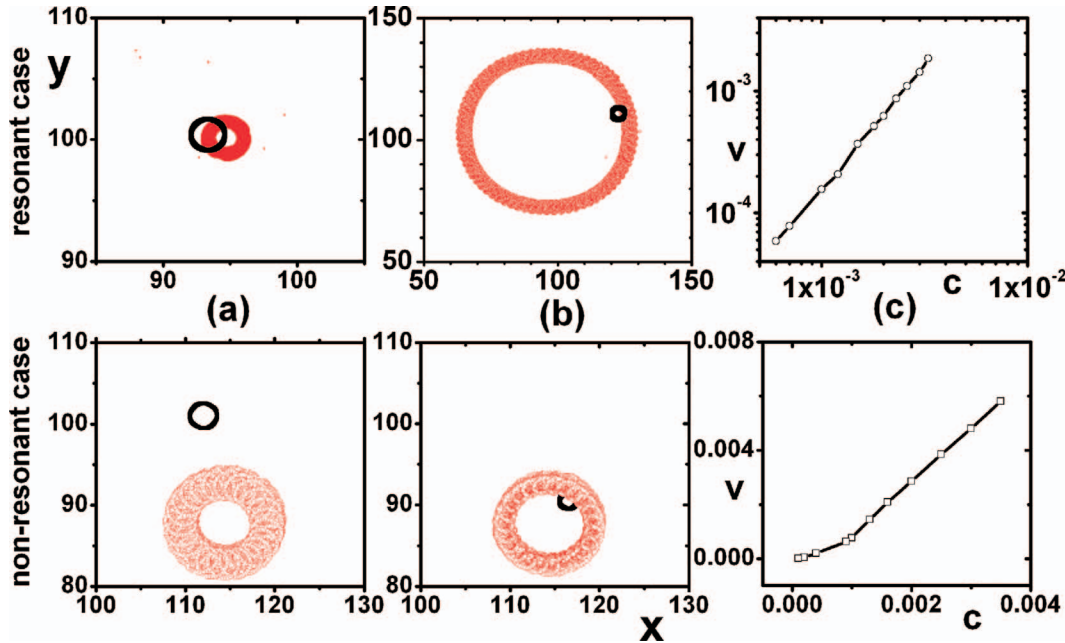


FIG. 3. (Color online) Nonresonant (resonant) case is shown in the top (bottom) panel. (a) The tip trajectories of subsystem 1 [$b_1=-0.045$ and $\epsilon_1=0.012$ in nonresonant case (discretization $dx=0.3/2$ and $dt=0.015/4$ in numerical simulation is used in this case) and $b_1=-0.045$, $\epsilon_1=0.022$ in resonant case]. (b) The tip trajectories of subsystem 2 ($b_2=-0.045$ and $\epsilon_2=0.036$ in nonresonant case and $b_2=0.05$, $\epsilon_2=0.02$ in resonant case). The black [red (gray)] orbit represents the tip trajectory before (after) the coupling is switched on. (c) The drift velocity of the spiral tip against the coupling strength c .

results, of spiral wave drift for weak coupling strength. We modified the models [19] that produce the main feature of the spiral dynamics in order to take into account the effects of the interaction between subsystems:

$$\begin{aligned}\dot{r}_i &= e^{i\phi_i}(R_i\omega_i - z_i) + h(c)(r_j - r_i) + f(c, \omega_i, \omega_j)e^{-ig(c)\phi_j}, \\ \dot{z}_i &= [\mu - i\omega_{m,i} - (1 + i\alpha_i)|z_i|^2]z_i, \\ \dot{\phi}_i &= \omega_i \quad (i, j = 1, 2),\end{aligned}\quad (2)$$

where r_i are the positions of the tips in the complex plane and z_i are the complex variables describing the spiral meander. $\mu_i + i\omega_{m,i}$ are the eigenvalues associated with the meander modes. (In the absence of coupling, the stationary state $z=0$ is obtained for $\mu < 0$ and corresponds to a rigidly rotating spiral wave at frequency ω . For $\mu > 0$, the z variable undergoes Hopf bifurcation and leads to a meandering spiral wave with modulation frequency ω_m .) The second term introduced in the r equation where $h(c) = \gamma_1 c$ with $\gamma_1 \ll 1$ describes the interaction of the two spiral tips, which plays the role of trapping both tip trajectories onto concentric orbits. The third term in the r equation accounts for the periodic forcing exerted by the spiral wave in the other subsystem. We set the functions f and g as $f(c, \omega_1, \omega_2) = \alpha e^{\beta(\omega_2 - \omega_1)}$ and $g(c) = \gamma c^2$. Through some simple calculations, we obtain the drift velocities for the two spiral tips as $v_{d,i} \propto g(c)f(c, \omega_1, \omega_2)$ and the radius for the drift orbits as $R_d \propto f(c, \omega_1, \omega_2)$. The function $f(c, \omega_1, \omega_2)$ is chosen so as to ensure that the fast rotating spiral wave has a drifting orbit with a small radius and the slow one a large radius. The difference in the radius of the drifting orbits tends to zero when two spiral waves have the same rotating frequencies. The scaling of the drifting velocity against the interaction c depends on the functional form of g . Here we can only recover a power law with an exponent around 2 for the non-resonant case.

Now we give some rationales for the modified model. From numerical simulations, we know that the interaction between the two subsystems changes neither the rotation frequencies of the spiral waves nor the type of spiral dynamics. Thus it is straightforward that the z and ϕ equations are kept unchanged. Then, for isolated reaction-diffusion systems, the spiral dynamics satisfies the symmetry group E_2 , which requires the spiral wave to be invariant under the actions of rotation, reflection, and translation. When the two reaction-diffusion systems are coupled, the only invariance violated is rotation, since the rotating frequencies of the spiral waves in the two different subsystems are not necessarily the same. Nevertheless, the invariance under reflection and translation should be kept in the modified model. It is obvious that Eq. (2) is invariant under translation and reflection.

Before proceeding, we address the difference between the results presented above and those in previous works. The spiral wave drift has been a common phenomenon in reaction-diffusion systems, which can be induced by a domain boundary [20], inhomogeneity [21], constant external field [22], periodic wave trains [23,24], periodically forced spiral waves [25,26], and so on. The last two are more rel-

evant to our work though they differ from ours in the following sense. In the case of the spiral drift induced by periodic wave trains, the spiral wave and the source of the periodic wave trains coexist in one 2D system, and the spiral wave always drifts along a fixed direction. Moreover, the final state of such a drift is the elimination of the spiral wave by its exit from the domain if the frequency of the wave trains is larger than that of the spiral wave. However, the spiral drift studied here is a sustained phenomenon induced by the interaction between spiral waves located in different systems. In the case of periodically forced spiral waves, the tips of the spiral waves display rich dynamics such as resonance-induced drift, entrainment, and irregular response of the spiral tip's motion. Interestingly, the drifting dynamics of periodically forced spiral waves could be realized in a coupled two-layer system [26]. Compared to our model, a fundamental difference is that the interaction between two layers in Ref. [26] is realized by periodically changing a parameter of each layer, such as the excitability of an excitable medium. In our case, the interaction appears in each layer only as an additive term. Moreover, in Ref. [26], the communication between the two layers proceeds based on the dynamical information extracted at one point for each layer, which is also quite different from our model. As for dynamical behaviors, the tip trajectories in Ref. [26] are always dependent on the forcing strength in forced spiral waves, while the tip trajectories are not sensitive to the coupling strength in our case.

ESTABLISHMENT OF THE RELATIONSHIP BETWEEN THE LEADER AND THE FOLLOWER

For weak coupling strength, we know that the interaction between the two subsystems is manifested by the movements of the spiral tips. If the coupling strength becomes strong, we will see different wave dynamics. In particular, no matter whether the coupled systems are resonant or nonresonant, the two subsystems will play different roles in the collective dynamics: one subsystem becomes dominant and plays the role of a leader, while the other acts as a follower. To show this clearly, we first consider the nonresonant case with the parameters used in Fig. 2. The results for different coupling strength are presented in Fig. 4. For $c=0.008$, the spiral wave in subsystem 1 looks similar to that in the isolated system [see Fig. 2(c)]. However, the two successive snapshots for subsystem 2 show that its original spiral wave is already gone and a targetlike wave shows up. Interestingly, the trace of the spiral wave of subsystem 1 can be found in subsystem 2 on the background of the targetlike wave. Furthermore, the wave propagations of the two subsystems on prescribed lines are plotted, where we can clearly see the modulation of the wave propagation in subsystem 2 by that in subsystem 1. On increasing the coupling strength to $c=0.012$, we may also find that the spiral wave in subsystem 1 is modulated by the targetlike wave in subsystem 2. Such a modulation can be reflected in either the snapshot of the spiral wave or the spatiotemporal plot of the wave propagation. At the same time, the period and the wavelength of the targetlike wave in subsystem 2 are decreasing. On further increasing the coupling strength to $c=0.014$, the spiral wave of subsystem 1

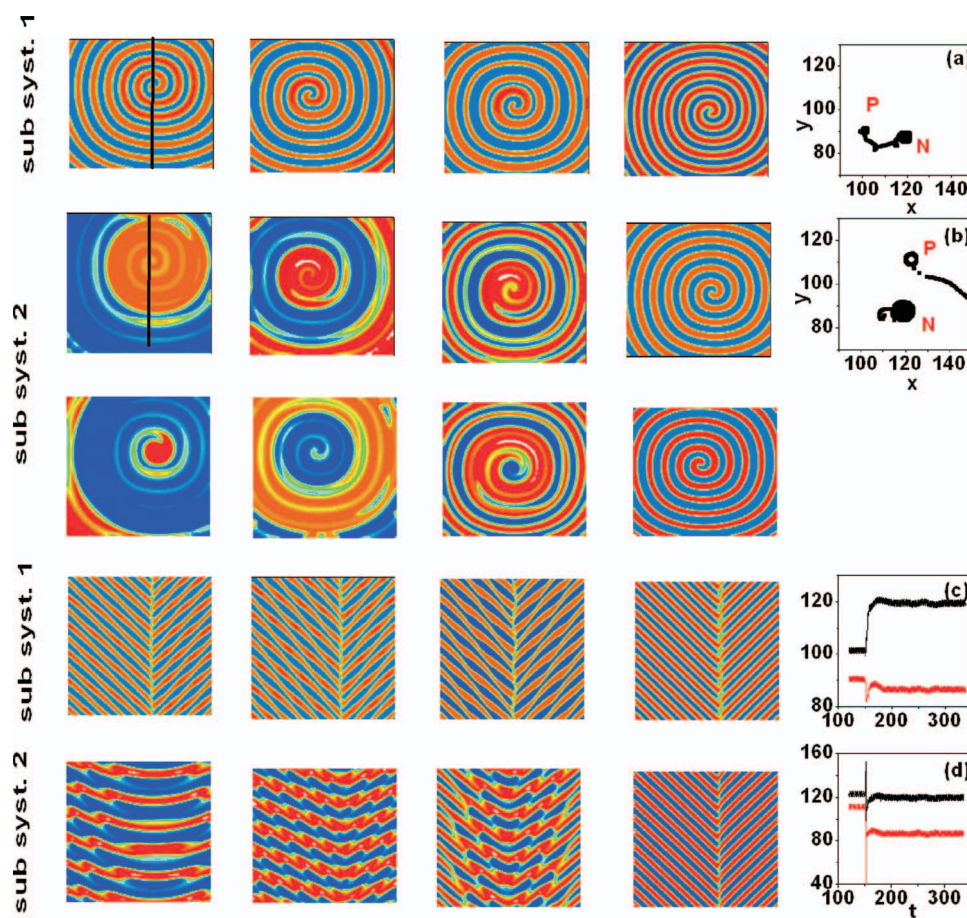


FIG. 4. (Color online) Transition process to phase synchronization where the relationship between the leader and the follower is established. The coupling strength c for the first four columns is $c=0.008, 0.012, 0.014$, and 0.02 , respectively. The top panels show snapshots for subsystem 1 for different coupling strengths. The following panels show successive snapshots for subsystem 2. The space-time plots (60 space units $\times 200$ time units, time increases from bottom to top) presented in the bottom two rows show the wave propagation in the two subsystems over lines crossing the spiral core in subsystem 1 (which are schematically shown in the top two panels for $c=0.008$). In the spatiotemporal plot, the time goes from bottom to top. Subsystem 1 is the one with $b_1=-0.045$ and $\epsilon_1=0.012$ and subsystem 2 has $b_2=-0.045$ and $\epsilon_2=0.036$. The rightmost column shows the tip trajectories for the two subsystems when $c=0.02$. To plot the tip trajectories, we first let the subsystems evolve freely for a while and then switch the interaction between the subsystems on. The tip trajectories on both sides of the switching time are plotted. (a) and (b) show the tip trajectories for subsystems 1 and 2, respectively. The symbol P (or N) refers to the steady tip trajectory before (or after) the interaction is switched on. (c) and (d) show the time series of the spiral tips' position for subsystems 1 and 2 [the red (gray) curve for the variable y and the black one for the variable x], respectively.

was generated in subsystem 2 except for the region of the spiral core. For sufficiently strong coupling strength, subsystem 2 is totally enslaved to subsystem 1 not only in the frequency but also in the wavelength, for example, the results shown in the column with $c=0.02$ in Fig. 4(d). In other words, phase synchronization between the two subsystems is built.

The process of the transition shown in Fig. 4 can also be demonstrated in the power spectra for the two subsystems (see Fig. 5). When $c=0.008$, both of the power spectra illustrate the coexistence of two components from the spiral wave in subsystem 1 and the targetlike wave in subsystem 2. The power spectra for $c=0.012$ show that in the dynamics of subsystem 2 the proportion of the spiral dynamics from subsystem 1 increases. The power spectrum for $c=0.014$ indicates that the spiral dynamics rooted in subsystem 1 begins to dominate the dynamics of subsystem 2. Finally, for suffi-

ciently strong coupling strength, only the component from subsystem 1 is left. It is also important to notice that the main frequency of subsystem 1 stays unchanged during such a process, which demonstrates the dominant role the subsystem 1 plays.

In the above example, subsystem 1 is the leader and subsystem 2 is the follower. The leader first drives the follower's spiral wave out of the domain, and then embeds its dynamics into its follower, and enslaves its follower when the coupling strength is strong enough. The different roles played by the subsystems are robust and cannot be interchanged by modifying the coupling strength or initial conditions in the non-resonant case. The scenario of establishing the relationship between leaders and followers can be found in the resonant case too. However, the roles played by the two subsystems can be changed through changes in the initial conditions of the coupled system. To show this, we consider the resonant

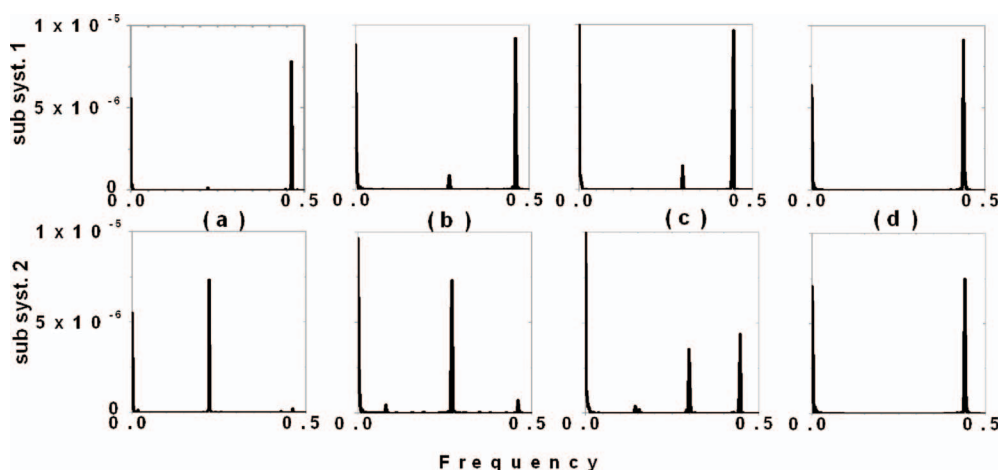


FIG. 5. Power spectra for the two subsystems when the relationship between the leader and the follower is being established. The parameters are the same as those used in Fig. 4. The top panel is for subsystem 1 and the bottom for subsystem 2. $c =$ (a) 0.008; (b) 0.012; (c) 0.014; (d) 0.02. It is clear that subsystem 1 takes over the dynamics of the subsystem 2 with increase of the coupling strength.

case used in the bottom panel in Fig. 3. As shown in Fig. 6, the subsystem with $b_1 = -0.045$ and $\epsilon_1 = 0.022$ plays the role of the leader, while the other with $b_2 = 0.05$ and $\epsilon_2 = 0.02$ becomes the leader in Fig. 7. The tip trajectories of the two subsystems in these two cases indicate that the reason the winner wins is that its spiral can survive the competition.

In the scenario where the leader takes control of the follower completely, there are several points to be addressed. (1) In the nonresonant case, the leader is the subsystem whose spiral wave rotates faster. Actually, the point is consistent with the drifting dynamics for weak coupling strength. When the coupling strength increases, the steady state where the slow rotating spiral wave settles its tip into a large orbit and the fast rotating spiral wave keeps its tip in a small orbit becomes unstable. Consequently, the slow rotating spiral wave explores more territory under the influence of the fast rotating spiral wave, and it is easier for it to drift out of the domain. During such a process, the rotation center of the fast rotating spiral does not shift its location too much. In the resonant case, the spiral tips of both subsystems move along the same large orbit for weak interaction. When the large orbit loses its capability for trapping spiral tips, the spiral waves in both subsystems drift violently. In such a case, whether one subsystem becomes the leader depends on whether it survives when its partner is pushed out of the domain. (2) The target wave appearing in the follower after its original spiral wave is gone is not generic. In the simulations, we have observed that the planar wave or other spatio-temporal chaos characterized by broader power spectrums. (3) When the coupling strength is strong, the leader's spiral wave may break up into several spiral wavelets while eliminating the follower's spiral wave. However, the coexistence of several spiral wavelets does not mean the defect mediates turbulence; instead the wavelets preserve the original dynamical properties of the leader as if it is isolated. Due to the limit in the model we used, the coupling constant cannot be too large; otherwise the local dynamics will be brought to a stable equilibrium and no pattern formation can occur any more. (4) Such a transition scenario is not limited to rigidly rotating spiral waves, and we can find them in other types of spiral dynamics. For example, we plot the results in Fig. 8 where a subsystem which displays spatiotemporal chaos or a meandering spiral wave is enslaved by a rigidly rotating spiral wave.

To get a general impression of the spiral dynamics in Eq. (1), we present the phase diagram on the plane of c and ϵ_2 in Fig. 9. To produce the phase diagram, we keep subsystem 1 unchanged, with parameters set as $b_1 = -0.045$ and $\epsilon_1 = 0.036$. Two types of media for subsystem 2 are considered: an excitable one with $b_2 = 0.05$ and an oscillatory one with $b_2 = -0.045$. From Fig. 9, we observe the definite appearance of three dynamical behaviors (spiral drift, phase synchroni-

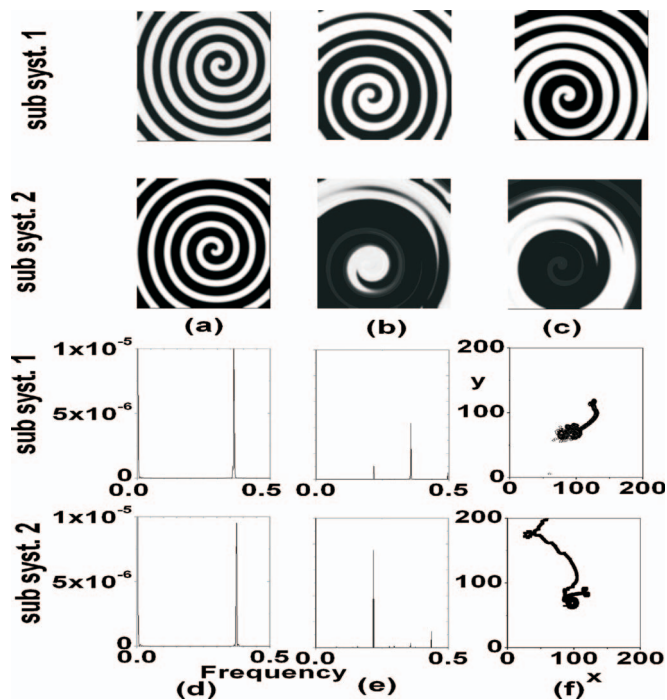


FIG. 6. Establishment of the relationship between the leader and the follower in the resonant case. Subsystem 1 is the one with $b_1 = -0.045$ and $\epsilon_1 = 0.022$ and subsystem 2 has $b_2 = 0.05$ and $\epsilon_2 = 0.02$. The coupling strength $c = 0.01$. The top two rows show the snapshots for subsystem 1 and subsystem 2, respectively. (a) Snapshots for the isolated subsystems. (b), (c) Snapshots at successive times for coupled subsystems. Clearly, subsystem 1 is a leader and subsystem 2 is a follower. (d) Power spectra for isolated subsystems. (e) Power spectra for coupled systems. (f) Tip trajectories for two subsystems when coupled. From the tip trajectories, we know that the spiral wave in subsystem 2 is flowing out of the domain while that in subsystem 1 stays forever.

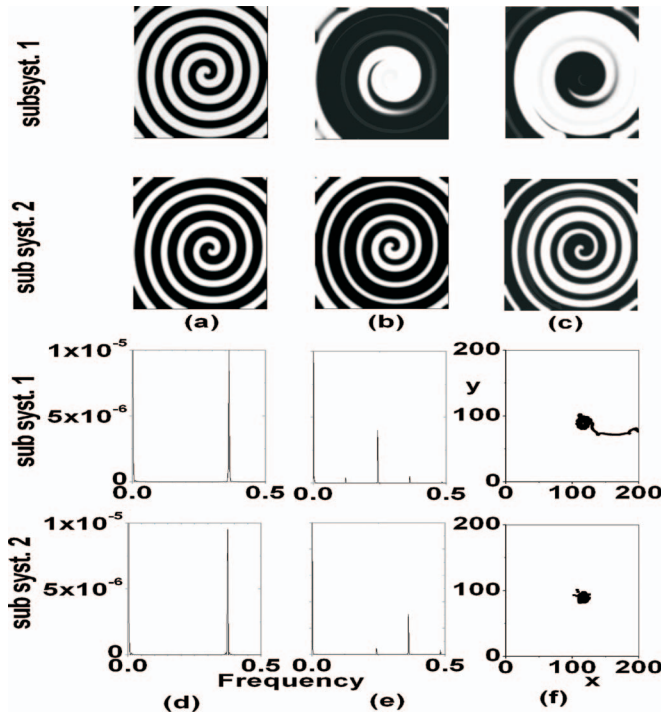


FIG. 7. Establishment of the relationship between the leader and the follower in the resonant case. The parameters are the same as in Fig. 6 but with different initial conditions. In this figure, subsystem 2 becomes dominant and subsystem 1 becomes a follower.

zation between the leader and the follower, and intermediate states). The critical curves separating the three dynamical regimes decrease with increasing ϵ_2 at first and then tend to be a little insensitive to the change of ϵ_2 .

Now, it is necessary to give a discussion of the model we studied. The question of interacting spiral waves in coupled reaction-diffusion systems has been considered in the literature [27]. For example, in Ref. [27], the authors discussed spiral dynamics in a two-layer lattice system. They found spiral synchronization for strong coupling strength and a transition process to synchronization as the coupling strength increases. However, different from our work, the coupled system considered in Ref. [27] consists of two identical layers and the synchronization they observed is different from ours. Furthermore, the preparation of the initial condition for coupled system is different from ours, which may explain why the drifting dynamics for weak coupling is ignored in Ref. [27].

Up to now, we have discussed the spiral dynamics in coupled reaction-diffusion systems. One question arises: How are these results related to three-dimensional systems? First of all, the system with two coupled layers can be taken as an approximation of a 3D system. Then consider the fact that in one 2D layer, the quantity Ddt/dx^2 appearing in the numerical simulation plays the role of coupling strength between adjacent nodes. We know that the thickness of the approximated 3D system is related to the coupling strength c by $L = \sqrt{Ddt/c}$. That is, two coupled layers with weak coupling constant refer to a thick 3D system. Therefore, we can get a naive correspondence between the spiral dynamics in a coupled two-layer system and that in the 3D case. Since in

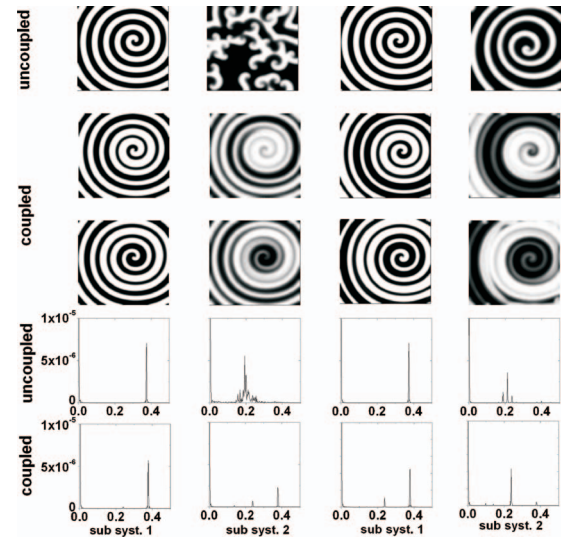


FIG. 8. Establishment of the relationship between the leader and the follower. Subsystem 1 is the one with $b_1 = -0.045$ and $\epsilon_1 = 0.012$. In the left two columns, subsystem 2 with $b_1 = 0.05$ and $\epsilon_1 = 0.075$ displays defect-mediated turbulence when isolated, while in the right two columns, subsystem 2 with $b_1 = 0.05$ and $\epsilon_1 = 0.065$ displays a meandering spiral wave. The top row shows the snapshot for uncoupled systems and the following two rows show the successive snapshots for the coupled systems, respectively. The bottom two rows show the power spectra for each subsystem when the systems are uncoupled and coupled, respectively.

the approximated 3D system the interaction between the fast rotating spiral wave and the slow one is realized by the diffusion of species u over a distance L , large L means that the influence of the fast spiral wave on the slow one is greatly weakened. As a result, the slow rotating spiral wave can keep its original functional form under the effect of the fast one. When L is small, the interaction between the fast and slow

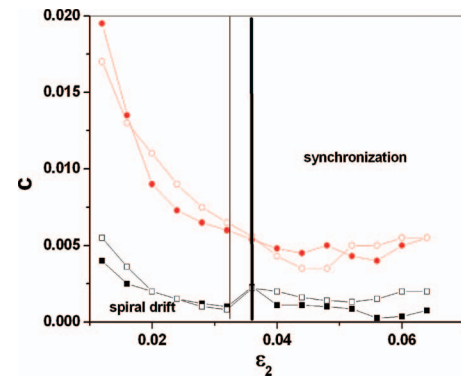


FIG. 9. (Color online) Phase diagram on the plane of c and ϵ_2 for the spiral dynamics in the coupled systems. Subsystem 1 is fixed with $b_1 = -0.045$ and $\epsilon_1 = 0.036$. Two types of subsystem 2 are considered: an excitable one with $b_2 = 0.05$ (the open symbols) and an oscillatory one with $b_2 = -0.045$ (the solid symbols). The regimes for three types of spiral dynamics (spiral drift, synchronization, and intermediate state) are shown. The bold (thin) line denotes the boundary of which subsystem is dominant for the oscillatory (excitable) case. For example, subsystem 2 (subsystem 1) dominates on the left (right) side of the bold or thin line.

rotating spiral waves is not weakened too much by the diffusion, and the continuous impact of the fast spiral wave on the slow one is equivalent to the establishment of a fast pace maker everywhere in the layer with slow spiral wave. As a result, we can expect the fast spiral wave to be dominant.

CONCLUSION

In this paper we have studied the spiral dynamics when two reaction-diffusion systems are coupled linearly. We find that the collective dynamics in coupled systems is strongly dependent on the coupling strength and the frequency mismatch. For weak coupling strength, the spiral waves in both subsystems stay unchanged like those in isolated systems in the aspects of frequency and wavelength. The interaction between the two subsystems is reflected by how spiral waves drift: when the frequency mismatch is large, the fast rotating

spiral keeps its tip trajectory close to the one when it is isolated, while the slow rotating spiral wave settles its tip down onto a large looped orbit; when the frequency mismatch is small, the tips of both spiral waves jump to the same large looped orbit. For large enough coupling strength, one subsystem will always dominate the other. When the frequency mismatch is large, the fast rotating spiral wave is the leader and will enslave the dynamics of its follower. If the frequency mismatch is small, which subsystem acts as leader depends on the initial condition of the coupled systems.

ACKNOWLEDGMENTS

The authors thank Professor Gang Hu for reading the manuscript. This work was supported by Grant No. 10405004 from Chinese Natural Science Foundation and a project sponsored by SRF for ROCS, SEM.

-
- [1] S. Jakubith, H. H. Rotermund, W. Engel, A. von Oertzen, and G. Ertl, *Phys. Rev. Lett.* **65**, 3013 (1990).
 - [2] A. V. Holden, *Nature (London)* **392**, 20 (1998).
 - [3] K. J. Lee, E. C. Cox, and R. E. Goldstein, *Phys. Rev. Lett.* **76**, 1174 (1996).
 - [4] R. E. Ecke, R. Mainieri, Y. Hu, and G. Ahlers, *Science* **269**, 1704 (1995).
 - [5] D. Barkley, *Phys. Rev. Lett.* **68**, 2090 (1992).
 - [6] A. Karma, *Phys. Rev. Lett.* **65**, 2824 (1990).
 - [7] M. Bär and M. Eiswirth, *Phys. Rev. E* **48**, R1635 (1993).
 - [8] A. Karma, *Phys. Rev. Lett.* **71**, 1103 (1993).
 - [9] Q. Ouyang and J. M. Flesselles, *Nature (London)* **379**, 143 (1997).
 - [10] M. Bär and M. Or-Guil, *Phys. Rev. Lett.* **82**, 1160 (1999).
 - [11] A. T. Winfree, *Science* **266**, 1003 (1994).
 - [12] Z. Qu, F. Xie, and A. Garfinkel, *Phys. Rev. Lett.* **83**, 2668 (1999).
 - [13] C. Zhang, H. Zhang, Q. Ouyang, B. Hu, and G. H. Gunaratne, *Phys. Rev. E* **68**, 036202 (2003).
 - [14] L. F. Yang and I. R. Epstein, *Phys. Rev. Lett.* **90**, 178303 (2003).
 - [15] S. Boccaletti, J. Kurths, G. Osipov, D. L. Valladares, and C. S. Zhou, *Phys. Rep.* **366**, 1 (2002).
 - [16] J. Yang, F. Xie, Z. Qu, and A. Garfinkel, *Phys. Rev. Lett.* **91**, 148302 (2003).
 - [17] For a meandering spiral wave, the secondary frequency f_2 is insensitive to the parameter ϵ in the Bär model. For example, $f_2=0.025$ for $b=0.05$.
 - [18] I. S. Aranson and L. Kramer, *Rev. Mod. Phys.* **74**, 99 (2002).
 - [19] D. Barkley, *Phys. Rev. Lett.* **72**, 164 (1994); B. Sandstede and A. Scheel, *ibid.* **86**, 171 (2001); H. Henry, *Phys. Rev. E* **70**, 026204 (2004).
 - [20] J. M. Davidenko, A. V. Pertsov, R. Salomonsz, W. Baxter, and J. Jalife, *Nature (London)* **355**, 349 (1992); V. N. Biktashev and A. V. Holden, *Phys. Lett. A* **181**, 216 (1993); J. Yang and M. Zhang, *Commun. Theor. Phys.* **45**, 647 (2006); H. Yang and J. Yang, *Phys. Lett. A* **365**, 204 (2007).
 - [21] M. Markus, Z. Nagy-Ungvarai, and B. Hess, *Science* **257**, 225 (1992); I. V. Biktasheva, *Phys. Rev. E* **62**, 8800 (2000).
 - [22] V. Krinsky, E. Hamm, and V. Voignier, *Phys. Rev. Lett.* **76**, 3854 (1996).
 - [23] G. Gottwald, A. Pumir, and V. Krinsky, *Chaos* **11**, 487 (2001).
 - [24] V. Krinsky and K. Agladze, *Physica D* **8**, 50 (1983).
 - [25] O. Steinbock, V. Zykov, and S. C. Muller, *Nature (London)* **366**, 322 (1993); V. Zykov, O. Steinbock, and S. C. Muller, *Chaos* **4**, 509 (1994).
 - [26] M. Seipel, F. W. Schneider, and A. F. Münster, *Faraday Discuss.* **120**, 395 (2001).
 - [27] V. B. Kazantsev, V. I. Nekorkin, D. V. Artyuhin, and M. G. Velarde, *Phys. Rev. E* **63**, 016212 (2001).